Letter of Intent for J-PARC

Spectroscopy of η mesic nuclei by (π^-, n) reaction at recoilless kinematics

K. Itahashi[a1], H. Fujioka[b2], S. Hirenzaki[c], D. Jido[d], and H. Nagahiro[e].

[a] *RIKEN Nishina Center, RIKEN, 351-0198 Saitama, Japan*
[b] *Department of Physics, The University of Tokyo, 113-0033 Tokyo, Japan*
[c] *Department of Physics, Nara Women's University, 630-8506 Nara, Japan*
[d] *Yukawa Institute for Theoretical Physics, Kyoto University, 606-8502 Kyoto, Japan*
[e] *Research Center for Nuclear Physics (RCNP), Osaka University, 567-0047 Osaka, Japan*

Abstract

We are interested in the recoilless production and spectroscopy of η mesic nuclei by using the (π^-, n) reaction. The K1.8BR beamline of the J-PARC will offer unique opportunity for the experiment. The goal of the present experiment is to understand the nature of the η meson in the nuclear medium, which is expected to couple to the $N^*(1535)$-nucleon hole, and to step forward to the chiral symmetry of the baryons.

1 Introduction

We consider recoilless production and spectroscopy of η mesic nuclei by using the (π^-, n) reaction. The target candidates at present are ^{7}Li and ^{12}C. The experiment comprises an entrance channel spectroscopy by the missing mass measurement and a decay channel spectroscopy by the invariant mass

[1]E-mail: itahashi@riken.jp
[2]E-mail: fujioka@post.kek.jp

measurement, thus realizes complete reconstruction of the reaction and decay kinematics in specified exclusive channels. The K1.8BR beamline of the J-PARC will offer unique opportunity for the experiment.

Recent studies [1–4] indicate strong coupling of the η-N system to the $N^*(1535)$ resonance (N^*) in threshold energies. Thus slow η in nuclear medium dominantly couples to N^*- nucleon hole (N^{-1}) thanks to the s-wave nature of the $\eta N N^*$ coupling, and hence the N^* properties are strongly reflected in the η-nucleus potentials. There are two major models for the N^* in nuclei, either as a quasi bound state of $K\Sigma$ or as a chiral partner of the nucleon. The two models predict much different η-nucleus potentials, and experimental examinations have been awaited for. The goal of the present experiment is to understand the nature of the η mesic nucleus and the in-medium N^* properties.

Our interests and motivations reside in the investigations of the QCD dynamics at the low energy limit by means of the spectroscopy of the η mesic nuclei. It is known that chiral symmetry plays an important role in this region, and hadrons dynamically gain the masses along with the decrease of the energy density of the vacuum in the hadron freezeout phase [5].

So far the experimental studies of the chiral symmetry have centered their weight in the in-medium meson properties. Discovery of deeply bound pionic states in lead [6–9] and following experiments reported the first quantitative estimation of the partial chiral symmetry restoration in the nucleus [10], and more systematic and precise experiments will be performed [11].

In contrast to the pionic atom experiment, the η in the present experiment is bound to the nucleus only by the strong interaction. This feature of the η mesic nuclei results in the large widths of the bound states and in the η-N – N^* coupling which involves a medium effect on the baryon, the N^*. Therefore the experiment we consider here may work as an alternative approach to the low-energy QCD theorem through the understandings of the chiral symmetry of the baryons [12, 13].

Experiments in another sector of this research field employ high-energy particle collisions to produce in-medium mesons and observe their decays. Reconstructing the invariant masses of the mesons, they reported observation of meson mass shifts due to the partial chiral symmetry restoration [14]. Several experiments are ongoing [15], and a few are in preparation following this line [16]. The advantage of the present experiment in this context is the small momentum transfer q, which is necessary for small ambiguity measurement. Large momentum transfer induces various processes in the nuclei besides meson production and inevitably introduces ambiguities. The prominent features of the present experimental technique are compared in Table 1.

2 Spectroscopy of η Mesic Nuclei

Comprehensive understandings of the atomic states of light mesons [17] stimulated motivations to pursue the structure of the heavier-meson bound nuclei and the feasibility of the experimental investigations. In this section, firstly, we briefly describe the current models of the η mesic-nucleus structures, namely i) chiral unitary model [18–21] and ii) chiral doublet model [12]. Details are found in the references. Secondly, we investigate the theoretically calculated (π^-, n) spectra based on the two models. The above two models predict much different spectral responses for the (π^-, n) spectra as shown in Fig. 1. The experiment is to distinguish them by the spectral shapes. Finally, we discuss decay modes of the η mesic nuclei and mention possible physical background based on the data from the previous experiments.

2.1 Theoretical Models

Theoretically η mesic nuclei were predicted first by Haider and Liu [22] and later studied more systematically by Chiang, Oset, and Liu [23]. It is widely accepted as characteristic features of the η mesic nucleus that the η-N system dominantly couples to $N^*(1535)(J^P = 1/2^-)$ at the threshold region [24]. The nature of the N^* itself needs a lot of discussion, and as for the in-medium properties of the N^*, there are roughly two classified trends in the theories. In the first "chiral unitary model" [18], N^* is a quasi-bound meson-baryon s-wave resonance of $K\Sigma - K\Lambda$ in analogous to the $\Lambda(1405)$, which is successfully described as a quasi-bound $\bar{K}N$ state [25]. If this is the case, we expect no mass shift of the N^* in the nuclear medium. The second "chiral doublet model" regards the N^* as the chiral partner of the nucleon [26]. In this case, the masses of the N^* and the nucleon decrease as the chiral symmetry restores and they degenerate at the full restoration as depicted in Fig. 2 [12]. With partial restoration of chiral symmetry in nuclear medium the mass difference of N and N^* is moderately reduced [27]. The potential of the η mesic nuclei depends strongly on the N^* and N masses as follows. In the case that the mass difference of N^* and N $(m_{N^*} - m_N)$ is smaller than η mass, the η potential has attractive nature and vice versa.

The calculated η-nucleus potentials for η-^{12}C system are shown in Fig. 3 [24, 28]. In the chiral unitary model, the potential shape is a simple Woods-Saxon type with the central depth of about 50 MeV [21]. In a good contrast, due to the above mentioned nature, the potential shape is more complicated for the chiral doublet model at the expected chiral order parameter $C = 0.2$ [28]. The potential shows a repulsive core at the interior of the nucleus and then an attractive pocket near the surface. Thus, predicted potentials are signifi-

cantly different. The binding energies B_η and widths Γ_η for the η in carbon[3] are estimated to be $(B_\eta, \Gamma_\eta) = (9.7, 35.0)$ MeV [20] and (90.1, 26.6) MeV[4] [29] for chiral unitary and chiral doublet models respectively.

2.2 (π^-, n) Reaction

The formation cross section of the η-mesic nuclei is calculated in detail in Ref. [24, 28–30]. There, the reaction cross section is expressed with the impulse approximation as

$$\left(\frac{d^2\sigma}{d\Omega dE}\right)_{^7\mathrm{Li}(\pi^-,n)^6\mathrm{He}\otimes\eta} = \left(\frac{d\sigma}{d\Omega}\right)^{\mathrm{lab}}_{p(\pi^-,n)\eta} \times S(E) \tag{1}$$

where $(d\sigma/d\Omega)^{\mathrm{lab}}_{p(\pi^-,n)\eta}$ is the elementary η production cross section in the laboratory frame and $S(E)$ is the nuclear response function. The response function is calculated by using the Green function method [31] with the distortion factor estimated by the eikonal approximation.

Figure 4 shows the total cross section of the elementary reaction $p(\pi^-, n)\eta$ with different incident momenta [32]. The cross section maximizes to be about 3 mb at $p_\pi = 700 \sim 800$ MeV/c. According to the differential cross section measurement at $p_\pi = 747$ MeV/c, the angular distribution is almost flat.

The η mesic nuclei formation cross section is maximized at the recoilless condition. Figure 5 depicts the calculated momentum transfer of the (π^-, n) reaction at the forward zero degree with changing the incident pion beam momentum for the three different η binding energies. As seen, the momentum transfer becomes zero at the magic momentum $p_\pi = 780$ MeV/c in case of $B_\eta = 50$ MeV. The magic momentum depends on the η binding energy, and the cross section enhancement can be tuned by varying the incident momentum.

The calculated cross sections for the η-mesic nuclei in the ^{7}Li(π^-, n) reaction are shown in Fig. 1 for the case of the infinite experimental resolution. The left panel is for the chiral unitary model and the right one for the chiral doublet model. The ordinate is the differential cross section and both models give the η mesic nuclei formation cross section of 25–50 μb/(sr MeV). The abscissa $E_{\mathrm{ex}} - E_0$ is the excitation energy of the reaction product measured

[3]Chiral unitary model calculated η-^{12}C and chiral doublet does η-^{11}C. However, difference is not substantial.

[4]The values for the chiral doublet model are obtained by solving the Klein-Gordon equation on the assumption that the N^* width on the complex plane is the same as that on the real axis. More realistic estimation will be given in the future.

from the threshold η production with a proton hole of $(0p_{3/2})_p^{-1}$. Since the level widths are larger than the level spacings between the couples of the η–p^{-1}, the spectral shapes will be not observed as simple Lorentzians. The strength is decomposed to several η–p^{-1} components and the largest contribution comes from the $s_\eta \otimes (0s_{1/2})_p^{-1}$ for the case of the ^{7}Li target. Theoretical calculations show similar spectra for the carbon with higher contribution from $s_\eta \otimes (0p_{3/2})_p^{-1}$.

As seen in the figure, the chiral unitary model shows its unique strengths in the relatively deeply bound region of $E_{\rm ex} - E_0 < -50$ and a bump in the $E_{\rm ex} - E_0 \sim 50$ region. We measure the overall structure of the (π^-, n) spectra, compare them to the theoretical predictions, and determine which model is in reality.

Major charged decay modes of the η in the vacuum are $\pi^+\pi^-\pi^0$ (23 %) and $\pi^+\pi^-\gamma$ (5%) [33]. Since the η is implanted in the nuclear medium and is coupled to the N^*, we consider that the decay modes of the η mesic nucleus is similar to that of the N^*. The major decay modes of $N^*(1535)$ are $N\pi$ $(35 - 55\%)$ and $N\eta$ $(30 - 55\%)$ [33] and the latter channel is energetically closed hence the $N\pi$ must be dominant.

Above theories calculate the signal η mesic nuclei formation cross sections and do not consider background. Possible source of the background will be π production in the (π^-, n) reaction. Figure 6 shows the measured inclusive proton energy spectra in the (π^+, p) reaction [34] for four targets of lithium, carbon, oxygen, and aluminum with the incident π^+ momentum of 800 MeV/c at the forward 15 degree in the laboratory frame. The arrows show the η production thresholds and the right side is the bound region. Note that the momentum transfer in the experiment is about 200 MeV/c at the finite angle. The spectral strength is located on large structureless continuum of about 130 μb/(sr MeV) in case of the lithium target. The spectra show structures in the unbound region, which are consistent with the theoretical models.

3 Experiment

One of the advantages of the present experiment over the above described previous one [34] is that the adoption of the (π^-, n) reaction opens new possibilities to perform the η mesic nucleus spectroscopies under the recoilless conditions at the forward zero degree. Realization of the small momentum transfer condition is indispensable to achieve better understandings of the physics. The other advantages are as follow. We measure the charged decay particles in the final states, and this enables full reconstruction of kine-

matics in several channels. Compared with the inclusive measurement, the background contribution will be drastically reduced in the exclusive measurement. However, the estimation of the reduction performance is beyond scope of this letter and will be given elsewhere. We also note that invariant mass measurement of $p\pi^-$ produced in the in-medium N^* decay may offer very unique information on the chiral symmetry of baryons.

3.1 Conceptual Design

The present experiment provides i) (π^-, n) reaction to produce the η mesic nuclei, ii) neutron measurement to make the missing mass spectroscopy, and iii) decay particle measurement for the invariant mass spectroscopy and for the exclusive channel tagging.

Simultaneous observation of the missing mass spectra at the recoilless kinematical conditions and the invariant mass spectra is realized by coincidence measurement of the particles in the formation channel (π^-, n) and those in the decay channels of the η mesic nuclei.

We measure the Q-value (Q) of the (π^-, n) reaction to deduce the mass of the reaction product. The Q-value is related to the binding energy of the η (B_η) as

$$\begin{aligned} -Q &= T_\pi - T_n & (2) \\ &= m_\eta - B_\eta + S_p(j_p) - [M_p + m_\pi - M_n], & (3) \end{aligned}$$

where T_π and T_n are the energies of the π^- and the neutron, respectively, $S_p(j_p)$ denotes proton separation energy in the target, and m_η, M_p, M_n and m_π are η, proton, neutron and π^- masses, respectively. We measure the energy of the neutron, convert it to the missing mass spectrum, and compare the spectrum to the theories.

We also measure the invariant mass of the η mesic nuclei in the observation of the charged decay particles. As described above, a charged decay candidate is $\pi^- p$. The Q-value of the N^* decaying into $\pi^- p$ is about 460 MeV which corresponds to the momentum of about 470 MeV/c. The in-medium N^* brings momentum of an order of Fermi momentum p_f and thus the produced $\pi^- p$ will be emitted nearly back-to-back with very high momenta of about 500 MeV/c.

The above observation of the charged particles serves also as very effective tagging of the exclusive decay channel of $\pi^- p$. Since the free decay of the η will not directly yield $\pi^- p$, quasi-free component observed in the missing mass spectra will be suppressed. The major background of π production will also be suppressed in the exclusive measurement.

3.2 Experimental Apparatus and Expected Spectra

The experimental site is the K1.8BR beamline of the J-PARC. The incident π^- central beam momentum is about 780 MeV/c, which will be varied for optimization and for covering wider ranges. The incident momentum will be either measured or controlled by the momentum slits in order not to deteriorate the missing mass resolution. Figure 7 shows the overview of the experimental apparatus. See Ref. [35] in detail since almost all the equipments are inherited from the experiment "J-PARC E15: A search for deeply-bound kaonic nuclear states by in-flight ^{3}He(K^-, n) reaction". The experimental setup around the target is shown in Fig. 8. We compare present experimental conditions to E15 in Table 2.

The incident π^- is measured by the beamline drift chambers (BDC) and by several beam defining counters (BDF) of lucite Cherenkov and scintillation counters. The emitted neutron in the (π^-, n) reaction with the similar momentum to the incident π^- is measured by the scintillation counter wall (NC) located at about 12 meter downstream of the target in the forward 0 degree while the incident beam and charged particles are bended off by the sweeping magnet.

The neutron momentum is measured by the time-of-flight in the 12 meter distance to the NC. The NC is consisted of the 112 = 16 (row) $\times$ 7 (layer) scintillation counters and charged-particle-veto counters. Each scintillation counter has a scintillator with the dimension of $20 \times 5 \times 150$ (cm) and two PMTs attached to the both ends and has time resolution of about 120 ps (σ). The expected missing mass resolution of the (π^-, n) reaction product is about 20 MeV/c^2 in FWHM at the central region of interest.

The target is surrounded by a cylindrical detector system (CDS) with the solid angle of about 2.5π sr situated in a solenoid magnet. The CDS has a radial tracking region (CDC) between the radius from r = 15 to 48 cm and scintillation counter hodoscope (CDH) outside of the CDC. The produced magnetic field has a good homogeneity of less than about ± 2 % within the tracking volume with 0.7 Tesla at the maximum. Rough estimation of the invariant mass resolution tells about 40-50 MeV/c^2 in FWHM at the 0.5 Tesla magnetic field. The incident π^- beam intensity is about 2 MHz during the extraction. The trigger of the data acquisition is defined as BDF $\otimes$ NC $\otimes$ CDH.

Figure 9 shows the expected missing mass spectra with the inclusive measurement of the ^{7}Li(π^-, n) reaction. The signal strengths were taken from Fig. 1. The abscissa is the excitation energy of the reaction product measured from the threshold η production with a proton hole of $(0p_{3/2})_p^{-1}$. We fixed the energy resolution to 20 MeV (FWHM) in the whole energy range.

The magnitude of the structureless background is taken from the past experiment of Chrien [34] and here we assume constant background of 90 μb/(sr MeV). Note that in reality, inclusive measurement may encounter difficulties of too high trigger rate and that major part of the background is expected to be suppressed in the exclusive measurement of the $\pi^- p$ decay channel. Even in the inclusive measurement, a hint of the bound state formation can be observed and the two models can be distinguished.

4 Summary

Since the major experimental equipment will be developed and constructed for the J-PARC E15 experiment, this experiment does not require dedicated R&D. Thus, the experiment is suitable in the K1.8BR beamline after the experiment E15.

The experiment simultaneously comprises missing mass and invariant mass spectroscopy of the η mesic nuclei. The momentum transfer of the reaction is optimized to be about zero. The tagging of the decay particles will be effective to perform exclusive measurement for better S/N ratio. The expected spectrum shows prominent performance of the experiment to distinguish between different models of the in-medium properties of the N^* .

Acknowledgments

We thank Dr. Ohnishi for providing us with necessary figures for the E15 setup and parameters. We are grateful to Drs. Outa, Suzuki, and Okada for stimulating discussions.

Tables

	Present Experiment	High $\sqrt{s}$ collisions
q/p_f	< 1	$\gg 1$
Hadron property	Meson or baryon	Meson
Hadron state	Quantum state	Relative motion in media
Medium state	Ground/excited	Hot/dense (not defined)
Spectroscopy	Missing + invariant mass	Invariant mass
Ambiguity	**Small**	Large

Table 1: Comparison of the present experiment and high-energy beam collision experiments. The present experiment has an advantage of small ambiguities.

	Present Experiment	J-PARC E15
Beam	π^-	K^-
Beam momentum	$0.7 \sim 1.0$ GeV/c	$1.0 \sim 1.1$ GeV/c
Reaction	(π^-, n)	(K^-, n)
Target	^{7}Li, ^{12}C	^{3}He
Momentum transfer	~ 0 MeV/c	$200 \sim 300$ MeV/c
Neutron momentum	$0.7 \sim 1.0$ GeV/c	$1.2 \sim 1.4$ GeV/c
Decays in interest	$N^* \to p\pi^-$	$K^-pp \to \Lambda p$, $\Lambda \to p\pi^-$
Typical decay momenta	~ 500 MeV/c	~ 500 MeV/c

Table 2: Comparison of the present experiment and E15 [35]. They have very similar experimental conditions.

Figures

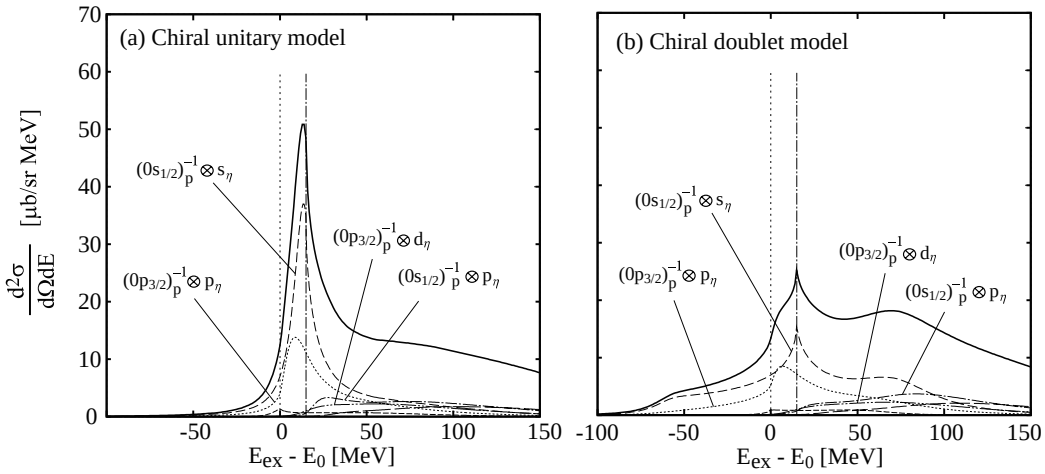

Figure 1: Calculated η mesic nuclei formation cross sections for the chiral unitary model(left) and the chiral doublet model(right) [29]. The left side is the bound region.

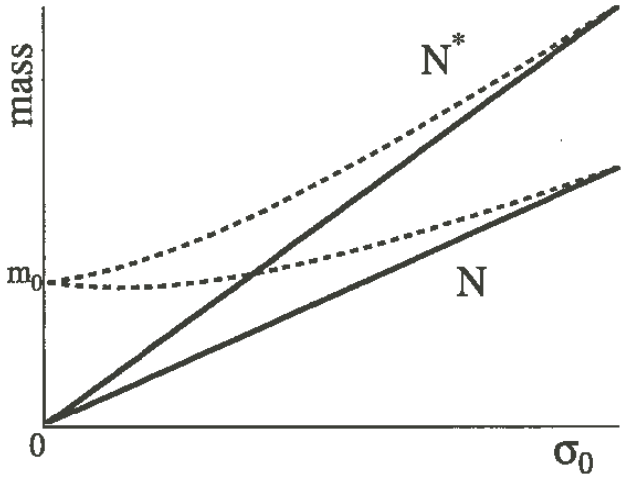

Figure 2: Change of the masses of the nucleon and the N^* depending on the chiral order parameter σ_0 [12]. The N and N^* degenerate at the full restoration of the chiral symmetry.

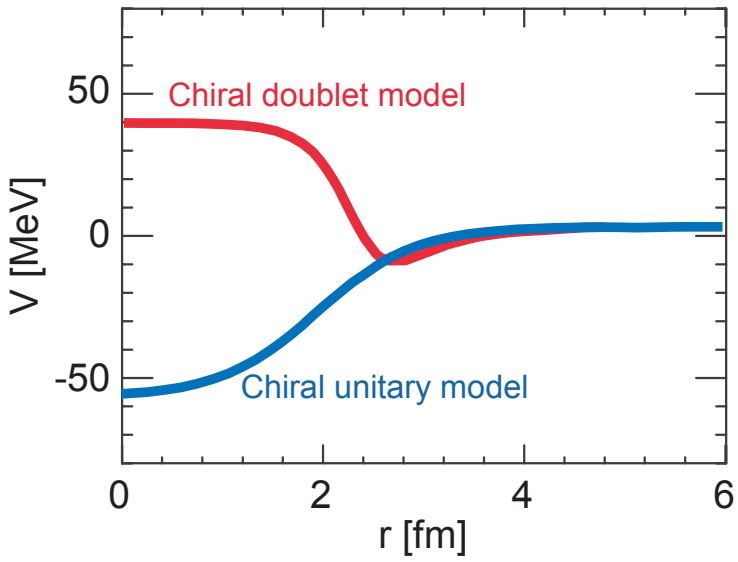

Figure 3: Calculated η-nucleus potentials for η-^{12}C system measured from the nuclear center [24,28]. The blue curve is for the chiral unitary model and the red for chiral doublet model.

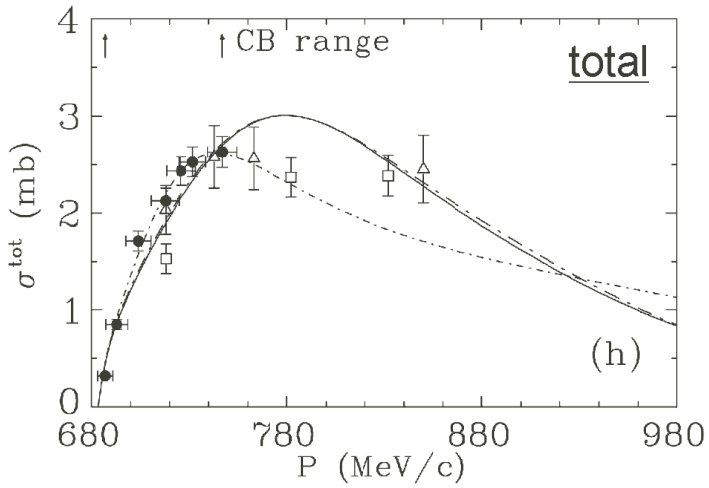

Figure 4: Elementary reaction cross section of $p(\pi^-, n)$ with changing the incident π^- beam energy [32].

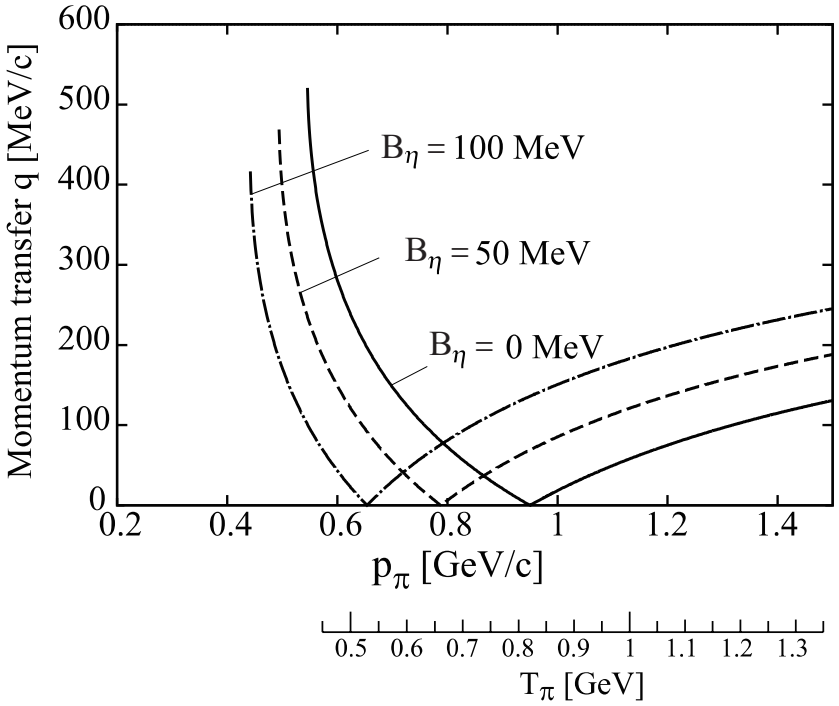

Figure 5: Momentum transfer of the (π^-, n) reaction with changing the incident beam energies for three different η binding energies.

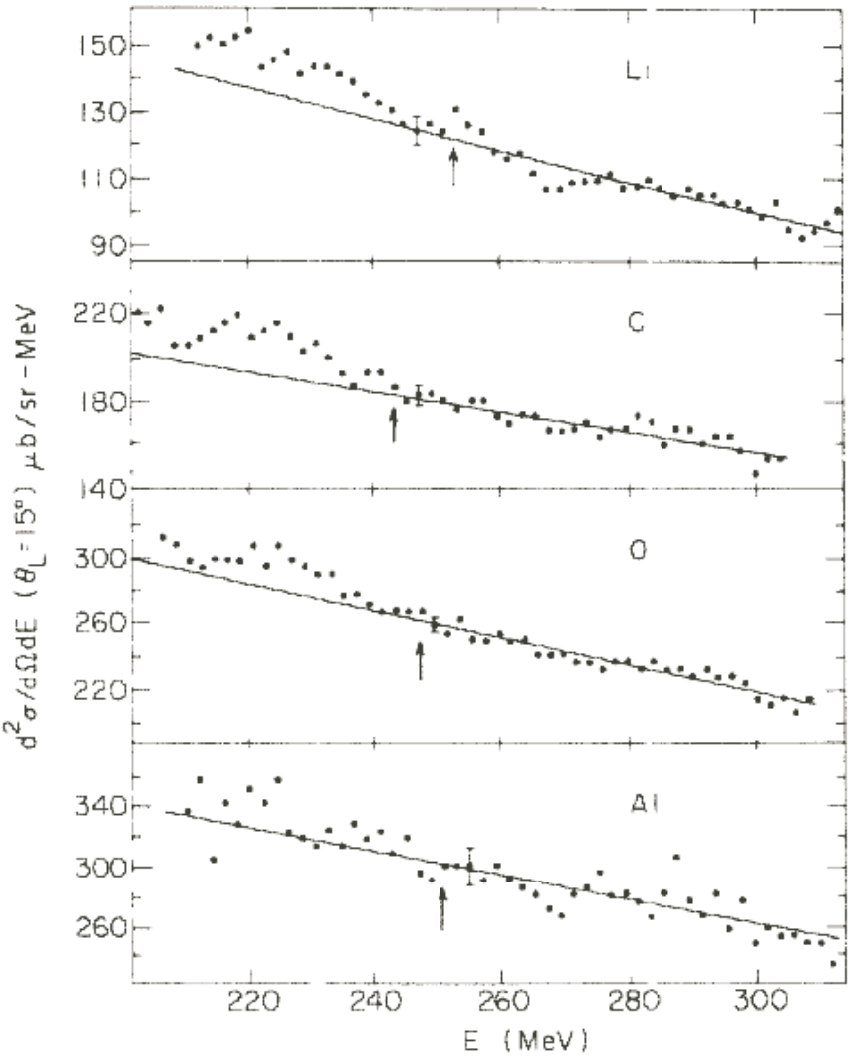

Figure 6: Measured differential cross sections of (π^+, p) reaction for lithium, carbon, oxygen, and aluminum targets with the incident π^+ momentum of 800 MeV/c at the forward 15 degree [34]. The η production thresholds are shown by the arrows. Right side is the bound region.

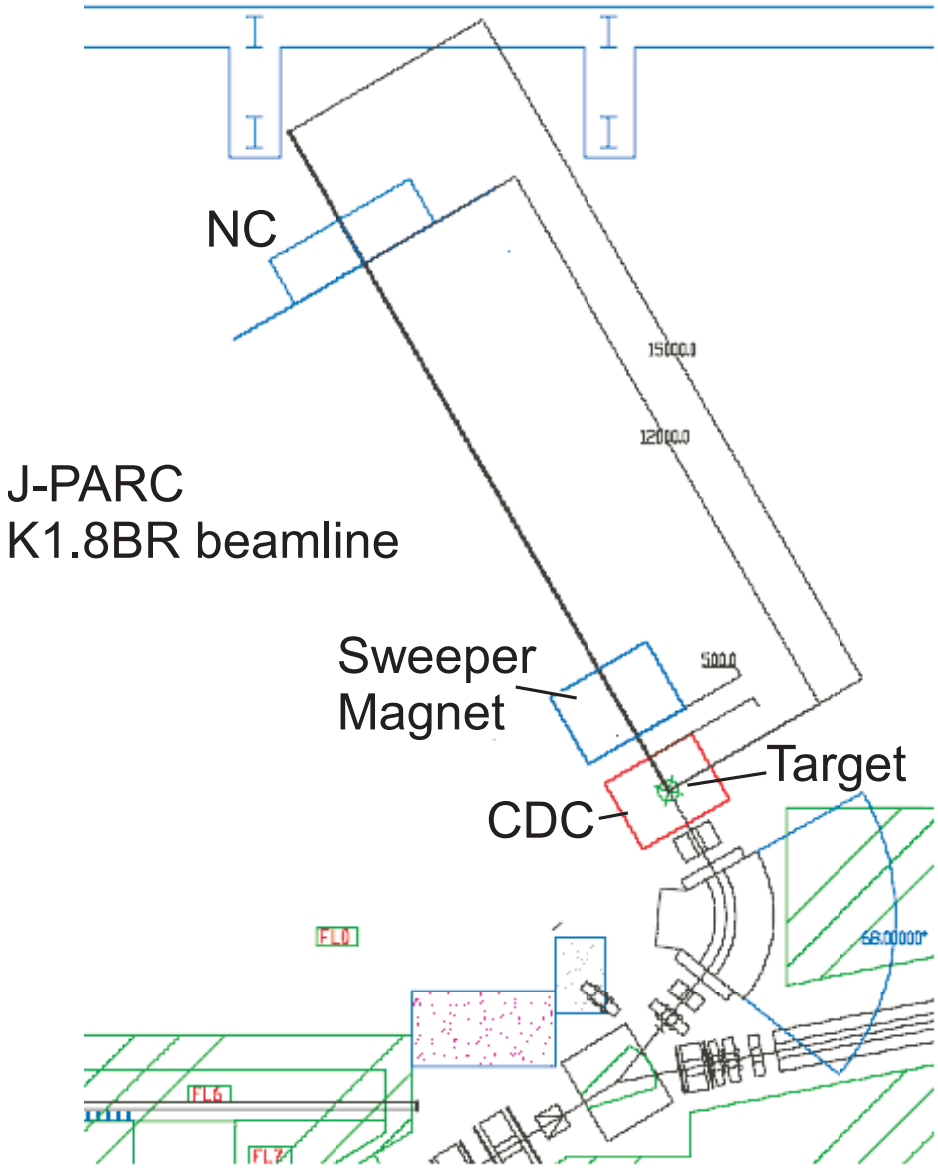

Figure 7: K1.8BR area and overview of the experimental apparatus [35].

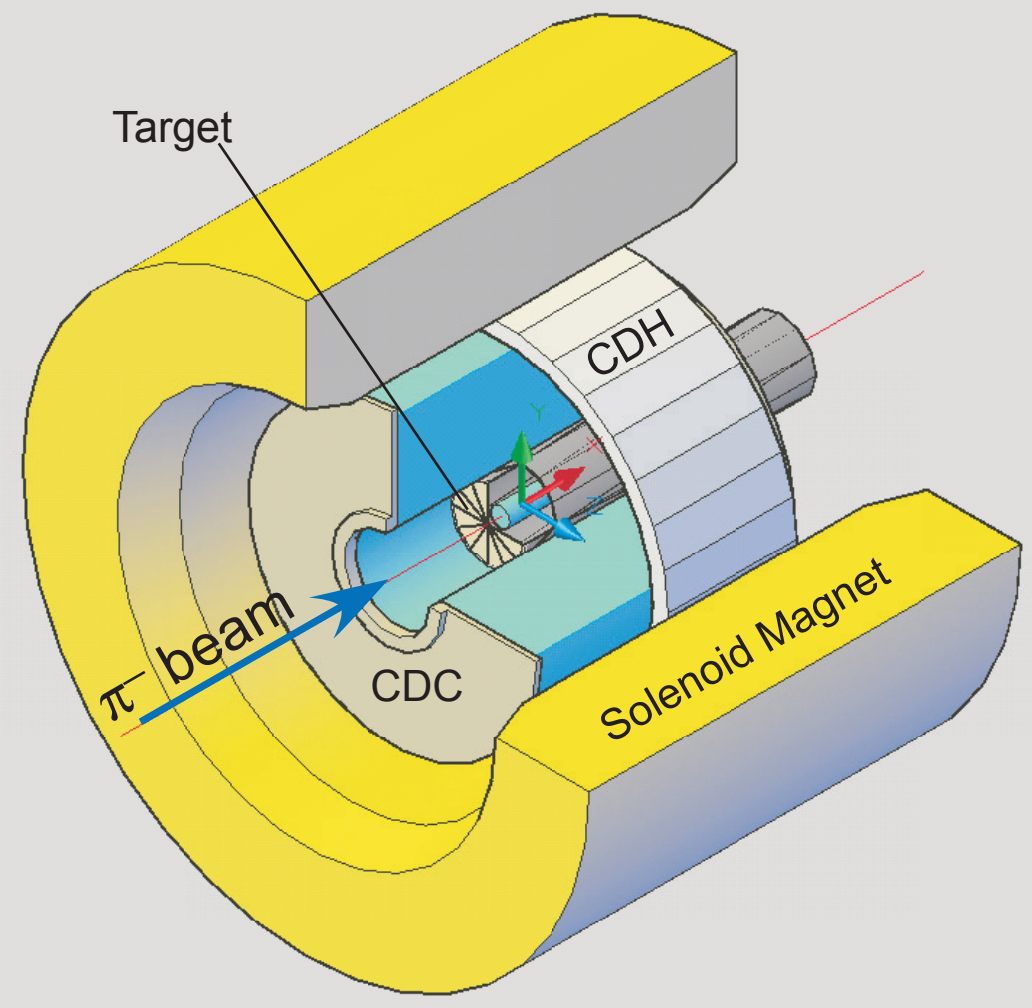

Figure 8: Close view of the experimental setup around the target [35]. The target is surrounded by the cylindrical drift chamber (CDC), the cylindrical detector hodoscope (CDH), and the solenoid magnet.

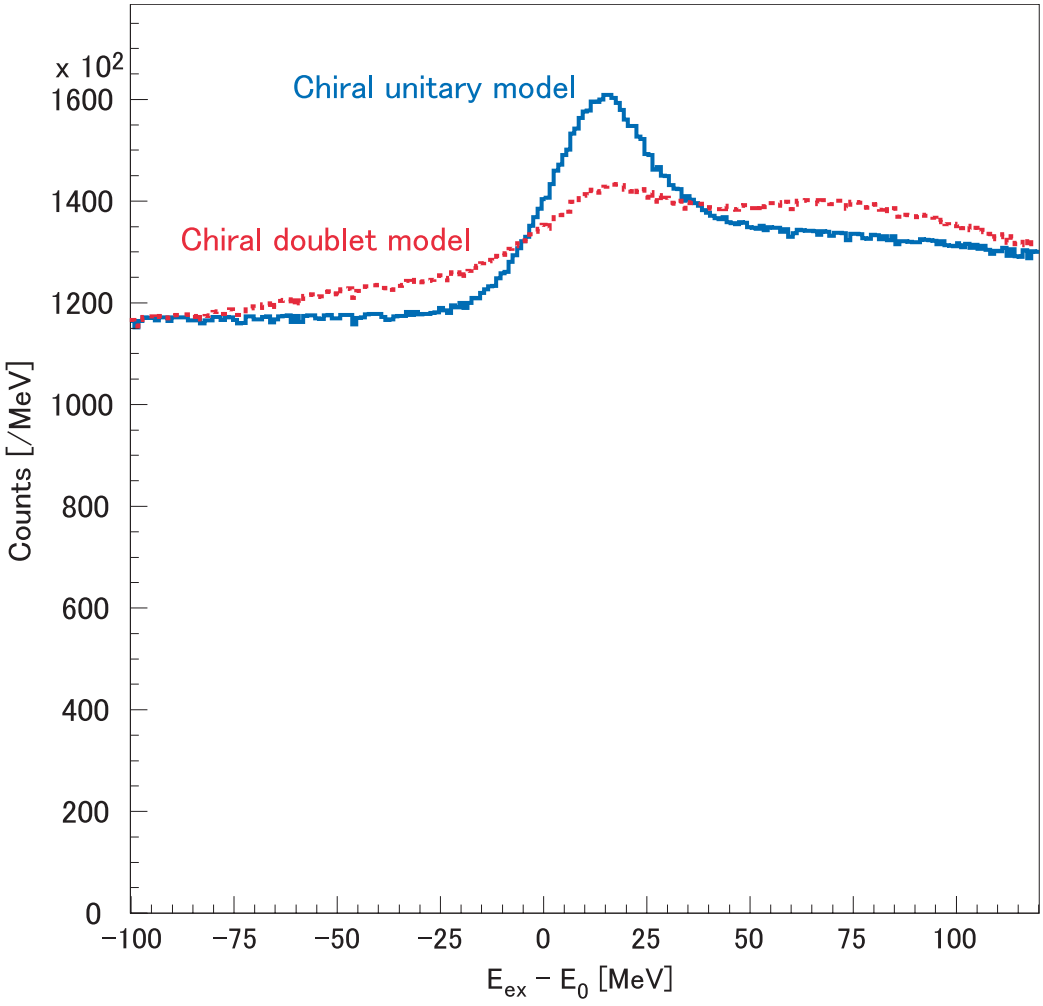

Figure 9: Expected ^{7}Li(π^-, n) inclusive spectra for both chiral unitary and chiral doublet models. The abscissa is the excitation energy of the reaction product measured from the threshold η production with a proton hole of $(0p_{3/2})_p^{-1}$. The experimental resolution is fixed to be 20 MeV in FWHM for the whole energy region (it is unrealistic for neutron measurement but we do not expect small structures outside of the central region). A constant background of 90 μb/(sr MeV) was assumed.

References

[1] W. Grein, P. Knoll, Nucl. Phys. **A338**, 332 (1980).

[2] R. S. Bhalerao, L. C. Liu, Phys. Rev. Lett. **54**, 865 (1985).

[3] B. Krushce *et. al.*, *ibid.* **74**, 3736 (1995).

[4] M. Benmerrouche, N. C. Mukhopadhyay *ibid.* **67**, 1070 (1991); Phys. Rev. **D51**, 3237 (1995).

[5] Y. Nambu and G. Jona-Lasinio, Phys. Rev. **122**, 345 (1961).

[6] T. Yamazaki *et al.*, Z. Phys. A **355**, 219 (1996).

[7] H. Gilg *et al.*, Phys. Rev. C **62**, 025201 (2000).

[8] K. Itahashi *et al.*, Phys. Rev. C **62**, 025202 (2000).

[9] H. Geissel *et al.*, Phys. Rev. Lett. **88**, 122301 (2002).

[10] K. Suzuki *et al.*, Phys. Rev. Lett. **92**, 072302 (2004).

[11] K. Itahashi *et al.*, RIBF proposal No.027 "Precision Spectroscopy of pionic atoms in $(d, {}^3\mathrm{He})$ nuclear reactions" (2007).

[12] D. Jido, Y. Nemoto, M. Oka, and A. Hosaka, Nucl. Phys. **A671**, 471 (2000).

[13] D. Jido, M. Oka, and A. Hosaka, Prog. Theo. Phys. **106**, 873 (2001).

[14] *for instance* R. Muto *et al.*, Nucl. Phys. **A774**, 723 (2006).

[15] *for instance* S. S. Adler *et al.*, Phys. Rev. C **69**, 014901 (2004).

[16] S. Yokkaichi *et al.*, Proposal for J-PARC P16 "Electron pair spectrometer at the J-PARC 50-GeV PS to explore the chiral symmetry in QCD" (2006).

[17] C. J. Batty, E. Friedman, and A. Gal, Phys. Rep. **287**, 385 (1997).

[18] N. Kaiser, P.B. Siegel, and W. Weise, Phys. Lett. **B362**, 23 (1995).

[19] T. Waas and W. Weise, Nucl. Phys. **A625**, 287 (1997).

[20] C. Garcia-Recio, T. Inoue, J. Nieves, and E. Oset, Phys. Lett. **B550**, 47 (2002).

[21] T. Inoue and E. Oset, Nucl. Phys. **A710**, 354 (2002).

[22] Q. Haider and L. C. Liu, Phys. Lett. **B172**, 257 (1986); Phys. Rev. **C34**, 1845 (1986).

[23] H. C. Chiang, E. Oset, and L. C. Liu, Phys. Rev. **C44**, 738 (1991).

[24] D. Jido, H. Nagahiro, and S. Hirenzaki, Phys. Rev. C **66**, 045202 (2002) and references therein.

[25] N. Kaiser, P.B. Siegel, and W. Weise, Nucl. Phys. **A594**, 325 (1995).

[26] C. Detar and T. Kunihiro, Phys. Rev. D **39**, 2805 (1989).

[27] H. Kim, D. Jido and M. Oka, Nucl. Phys. **A640**, 77 (1998).

[28] H. Nagahiro, D. Jido, and S. Hirenzaki, Phys. Rev. C **68**, 035205 (2003).

[29] H. Nagahiro, D. Jido, and S. Hirenzaki, *in preparation.*

[30] H. Nagahiro, D. Jido, and S. Hirenzaki, Nucl. Phys. **A761**, 92 (2005).

[31] O. Morimatsu and K. Yazaki, Nucl. Phys. **A435**, 727 (1985); Nucl. Phys. **A483**, 493 (1988).

[32] S. Prakhov *et al.*, Phys. Rev. C **72**, 015203 (2005).

[33] W. -M. Yao *et al.*, J. Phys. G **33**, 1 (2006).

[34] R. E. Chrien *et al.*, Phys. Rev. Lett. **60**, 2595 (1988).

[35] M. Iwasaki, T. Nagae *et al.*, Proposal for J-PARC E15 "A search for deeply-bound kaonic nuclear states by in-flight ^{3}He(K^-, n) reaction".